by H. F. Okorn-Schmidt

Characterization of silicon surface preparation processes for advanced gate dielectrics

This paper gives a short overview of issues associated with the surface preparation of silicon surfaces for advanced gate dielectrics and the appearance and nature of the wafer surface after different chemical treatments. The main portion of the paper demonstrates the use of electrochemical open-circuit potential (OCP) measurements as a simple and powerful technique to investigate and characterize wet silicon surface-preparation processes. This technique provides unique information about the evolution of semiconductor surface reactions in wetchemical environments and permits the investigation of the kinetics of oxidation and etching processes in situ and in real time. Very good agreement between results obtained by this technique and results from multiple internal reflection-Fourier transform infrared spectroscopy (MIR-FTIR), X-ray photoelectron spectroscopy (XPS), spectroscopic ellipsometry (SE), and contact-angle studies is presented in this paper. A model is also presented which permits the correlation of the

measured open circuit potential difference to the thickness of a growing native oxide. The etching behavior of an ultrathin thermally grown silicon oxide layer in hydrofluoric acid (HF) is discussed as a new result obtained using the OCP technique.

Introduction

Few semiconductor processing steps have attracted as much interest over the last decade as the gate dielectric formation and the prior surface preparation. In the early days of solid-state device technology, the importance of clean substrate surfaces was already recognized to have a critical impact on the performance of simple transistors on germanium [1]. Since that time, with the introduction of silicon as substrate material and the rapid progress made with it, contamination issues have become even more critical, resulting in the implementation of more effective wafer cleaning: traditional wet-chemical processes [2–6] and combinations with gas/vapor-phase dry processes [7]. As a result, much progress has been made in the last decade in defect reduction, with a focus on heavy metals, alkali, and other light elements, organic contamination,

Copyright 1999 by International Business Machines Corporation. Copying in printed form for private use is permitted without payment of royalty provided that (1) each reproduction is done without alteration and (2) the Journal reference and IBM copyright notice are included on the first page. The title and abstract, but no other portions, of this paper may be copied or distributed royalty free without further permission by computer-based and other information-service systems. Permission to republish any other portion of this paper must be obtained from the Editor.

0018-8646/99/\$5.00 © 1999 IBM

particles, and in general residues of any kind which are foreign to the surface. Now, with the rapid approach of advanced gate dielectrics only a few atomic layers in thickness, and also the increasing interest in high-k materials, new questions arise and expressions such as "materials foreign to the surface" take on a new meaning. For example, should native oxides or wet-chemically grown oxides, which are residues from the prior cleaning process, be considered as harmful and therefore stripped before any gate dielectric growth? Or, alternatively, can these oxides be grown in a clean, reproducible way to become a valuable part of the final dielectric material? Where is the "native" oxide located after dielectric formation: on top of a thermally grown dielectric (at the interface with the gate material) or at the silicon-substrate interface in the event that a dielectric is deposited on top? To be able to define optimized solutions for each individual problem, it is of critical importance to understand the surface chemistry of silicon and silicon dioxide (often referred to as silica) and to investigate and influence the physicochemical processes at the semiconductor/electrolyte interface. As gate dielectric formation on real devices takes place on structured wafers, optimizing the surface-preparation process becomes a multivariable problem, because questions involving chemical components, mixing ratios, maximum allowable treatment time, temperature, and tooling must be answered for multiple materials exposed simultaneously.

In this paper, a short overview is initially given of the appearance and nature of the silicon surface after different chemical treatments and the associated positive and negative aspects. In the main section, a powerful but simple technique for monitoring and characterizing silicon surface processes in wet-chemical environments (*in situ* and in real time) is demonstrated on the basis of a review of experimental results and recently published papers.

Chemical composition of the silicon surface

• Contamination issues

The chemical state of the silicon surface after a cleaning process can be either in an oxidized form or oxide-free, bare silicon, terminated by Si–H groups. Termination of the silicon surface with deuterium, halogens such as bromine and iodine, and alkoxy groups (Si–O–R, where R is an organic group) is also being investigated [8–12].

The silicon surface, after a wet cleaning step and a final oxidative step, appears hydrophilic; i.e., a layer of water is absorbed when the wafer is removed from an aqueous liquid such as de-ionized (DI) water. The thickness of this SiO₂ layer is between 0.6 and 2.0 nm, its nominal value depending on oxidation conditions and the measurement techniques used. This chemical oxide (often referred to as "native" oxide) forms a passivation layer with a dangling-

bond defect density in the range of 10¹² cm⁻² at the Si/SiO, interface [13, 14]. The defect densities reported are about two orders of magnitude higher than for thermal oxides. However, recent studies suggest that the quality of the native oxides is strongly dependent on the applied chemistry in which they are formed, and that higher-quality oxides can be obtained with alternate chemistries such as DI water/ozone [15-18]. Wet-chemical oxides protect the Si surface from some recontamination or at least render the surface less sensitive. On the other hand, such thin oxides left on the surface are detrimental, for example, to epitaxial silicon deposition and might become increasingly critical for subsequent thermal oxidation as the gate oxide thickness decreases. For such purposes, cleaning sequences which end with an HF step (i.e., processing with a native-oxide-free surface) might be preferred. Such a surface after HF cleaning is hydrophobic (i.e., aqueous liquids do not adhere to the surface), and the silicon dangling bonds are passivated with hydrogen atoms. The hydrogen passivation is very stable, and surface-state densities are extremely low.

• The hydrophilic surface—Si-(OH)

Unlike thermally grown oxides, which have been characterized quite extensively because of their technological significance, wet-chemical oxides are not very well understood; more thorough investigations have recently been undertaken [17, 18]. Wet-chemically grown oxides are hydrophilic in contrast to thermal oxides. This difference is caused by the way the oxygen atom is bound to the silicon on the surface. Thermal oxides are characterized through the formation of siloxane rings, which are very stable against hydrolysis. Wet-chemically grown oxides are generally covered with surface hydroxyl groups (Si-OH) called silanol groups, and are very similar in their behavior with respect to silica gels, which are used for metal adsorption (ion exchange resins), as a substrate for catalysts, and for other applications [19]. Geometrical considerations and chemical measurements indicate an average surface density of around five (typical range 2-12) hydroxyl groups per nm² [20]. It is important to note that not all hydroxyl groups formed on a surface are chemically equivalent owing to structural differences in their coordination, but in general the surface hydroxyl groups on a hydrous oxide have donor properties similar to those of their corresponding counterparts in solution, the hydroxides. The sorption of metal ions and protons can be understood as competitive complex formation with deprotonated surface groups (Si-O⁻) which behave like Lewis bases. This means that the adsorption of species on a hydrous oxide surface of Si can be compared with complex formation reactions in solution, as demonstrated by Schindler et al. [21]. However, the extent of adsorption also depends strongly on the surface charge of the oxide

352

(i.e., the number of hydroxyl groups and the degree of dissociation) and, obviously, on the pH of the solution. More recent studies are extensively investigating the interaction between metal contamination in liquid and the silica surface [22, 23].

Besides being responsible for metal contamination, the surface charge of wet-chemically grown oxides on a wafer surface is also responsible for particulate contamination. An excellent chemical particle-removal process is to increase pH in order to obtain a negative (and, to most particles), repulsive surface charge by deprotonating the surface silanol groups. However, because this negative surface charge is very attractive to metal contaminants, a good balancing of chemical processes is needed to remove both particulates and metals and to avoid their redeposition.

• The hydrophobic surface—SiH,

When the oxide layer from a crystalline silicon substrate is removed with HF, a hydrophobic surface with unique properties is obtained: i.e., having a good resistance to chemical attack and a low surface recombination velocity, which means a surface with a very low surface-state density. Since the late 1980s it has been accepted that such a surface is hydrogen-terminated instead of having F bonded to the Si atoms [24–29]. Although the mechanism is not completely understood, it is known that the etching of SiO₂ from a silicon surface occurs in two steps. First, the oxide layer (Si⁴⁺) is rapidly dissolved in HF, forming SiF₆²⁻ ions in solution, with the reaction rate dependent on the HF concentration. In the second step, anodic dissolution of the last monolayer of oxidized Si $(Si^{n+}$ with n = 1, 2, 3) occurs, resulting in a hydrogenpassivated Si surface with mainly dihydride species on the (100) surface and monohydride species on the (111) surface [26, 30, 31]. More details on the etching mechanism are discussed in this paper, in the section in which this reaction path is monitored in situ and in real time.

As has been mentioned, this hydrogen-passivated surface exhibits good stability over a period of hours, shows less organic recontamination than silica surfaces [32–34], and has fewer problems with metallic contamination. Only noble metals such as Cu and Ag can deposit electrochemically on the surface, which leads to a dramatic roughening of the surface [35–37]. In general, however, such problems are observed only rarely in a device fabrication environment because of the high dilution of HF with high-purity DI water. In addition, the plating of Cu onto silicon during the etching process can be prevented by adding a sufficient amount of HCl (hydrochloric acid) to the HF solution [38]. The major difficulty with having HF as the last processing step (HF-last processing) is the wafer rinsing and drying process.

In the pre-gate-oxidation preparation step, device wafers after HF processing have both hydrophobic and hydrophilic areas (mixed surfaces); also, the opened, active areas are not 100% H-passivated and have fluoride adsorbed. This requires very careful rinsing with DI water, which may slowly reoxidize the surface when it contains higher levels of dissolved oxygen. A very sophisticated drying process must also be applied [33, 39–41]. As another complication, surface-roughening effects introduced by the cleaning process must be considered, but so far no clear correlation to gate dielectric quality has been found [42, 43]. However, in the case of extreme surface roughness it has been shown recently that the tunneling current is increased, primarily because of the resulting oxide nonuniformity [44].

Considering the problems associated with hydrophiliclast cleaning (metal contamination, possible impact of native oxide on dielectric properties), HF-last cleaning sequences seem very attractive; it would be expected that improved gate reliability and oxide integrity could be achieved. However, so far experimental proof for the superiority of HF-last cleaning has not been reported [45]. This might be because of uncertainty involving the extent to which HF-last processing on structured wafers really results in H passivation, and, if so, how stable this passivation is. In fact, final H passivation requires a sufficiently long over-etch time, which is sometimes difficult to achieve, and, as mentioned earlier, requires an optimized rinsing and drying process. An effective measurement technique is needed in order to optimize surface-preparation processes such as HF etching and native-oxide passivation. Such a technique was introduced in 1995 [46-48]; it is based on measurement of the time evolution of the open-circuit potential (OCP) of a semiconductor surface when it is immersed in an electrolyte. Earlier work has already shown that characterization by electrochemical OCP measurements can assist significantly in optimizing wet etching of metals and silicides on top of silicon [49].

In the following, after a brief theoretical introduction, the applicability of OCP measurements in the study of wetchemical oxidation of Si by SPM ($H_2SO_4:H_2O_2=4:1$) and SC1 ($NH_4OH:H_2O_2:H_2O=0.25:1:5$) mixtures and the removal of the resulting oxides by HF and caustic mixtures are reviewed. A new application of this technique for investigating and characterizing the etching behavior of thermally grown ultrathin dielectric materials is demonstrated for the first time.

Theoretical considerations

Immersion of a semiconductor in an electrolyte which contains one or more redox couples results in a chargetransfer process between the two phases until electrostatic equilibrium (equality of the free energies of the electrons in both phases) is obtained or, in other words, until the Fermi levels $(E_{\rm F})$ in the solid and the solution become equal. This produces an electric field at the solid/liquid interface, causing the formation of an electrical double layer, as in the case of a metal electrode. But semiconductors differ from metals in the nature of their potentials and potential distribution in two important ways:

- 1. The electrochemical potential of electrons in a semiconductor can be varied over a wide range by the addition of a trace quantity of suitable impurity (e.g., p- or n-doping with boron or phosphorus, respectively).
- The dielectric constant of most semiconductors is in the range from 10 to 20. This, coupled with low free-carrier densities, enables such materials to support extensive space charges, in contrast to the behavior of a metal in this respect.

Under these conditions, two diffuse layers are formed at the interface when a semiconductor is immersed in an electrolyte: one in the electrolyte (Gouy layer) and the other in the semiconductor (space-charge layer). These two layers, together with an intermediate region (the Helmholtz layer), form the electrical double layer. The ions that form the electrolyte region of the double layer can approach the interface to the distance of the outer Helmholtz plane. Between this plane and the surface of the semiconductor exists a potential difference $\phi_{\rm H}$, the Helmholtz potential. This interface distance between charges corresponds to the ionic radius, including the solvating shell, and may be considered as a charged capacitor. The overall potential difference ϕ_{G_2} (Galvani potential) between the bulk of the semiconductor and the bulk of the electrolyte is given by the sum of the electrical potential differences $\phi_{\rm S}$ and $\phi_{\rm G}$ in both diffuse layers, and ϕ_H :

$$\phi_{Ga} = \phi_{S} + \phi_{H} + \phi_{G}. \tag{1}$$

The Gouy layer is a diffuse space-charge region extending out from the electrode. Its thickness becomes negligible and indistinguishable from the Helmholtz double layer for moderate ion concentrations. Therefore, if the electrolyte solution is concentrated, above $\sim\!10^{-2}$ M, $\phi_{\rm G}$ (the potential drop in the Gouy layer) is negligible [50]. This simplifies the model; the potential drop may occur entirely within the semiconductor $(\phi_{\rm S})$ or within the electric double layer in solution $(\phi_{\rm H})$. However, in practice the potential drop occurs partly in the semiconductor and partly in the Helmholtz layer, so that there are two processes that must come to equilibrium—electron exchange and adsorption/desorption of ions. It is experimentally found that the potential drop across the Helmholtz double layer is sensitive to the electrolyte

composition and is therefore determined by the absorption/desorption of ions, especially in the case of an insulator surface (i.e., SiO₂). On the other hand, the Helmholtz double layer shows an insensitivity to electron transfer which is related to its thickness of only 1/100 to 1/1000 the thickness of the space-charge layer. Therefore, if charge is transferred from the bulk to the surface, giving a voltage change, or if a voltage is applied, only a small fraction of the voltage change appears in $V_{\rm H}$, but, instead, is distributed over the space-charge layer. The role of the space-charge layer in the semiconductor is to adjust the carrier concentration at its surface in order to make the net rate of electron transfer between the involved band and the redox couple in the electrolyte equal to zero. This is achieved by bending of the conduction and valence band relative to the flat-band potential, which is the potential at which no space-charge layer exists. Additional complications arise because charges on the semiconductor side of the interface may also exist in surface states, which are energy states located at the surface within the bandgap. However, this potential drop is distributed over the total interface, Q. Any variations of the overall voltage developed by this electrochemical cell can be measured against a reference electrode at open circuit with a highimpedance voltmeter, so that negligible current can flow through the cell. In such a measurement setup, additional potential drops are involved at the electrolyte/reference electrode, reference electrode/metal, and semiconductor/ metal interfaces. The semiconductor/metal interface is an ohmic contact; i.e., the potential distribution at this contact remains unchanged during any variations of the electrode potential and also the potential drops at the other two additional barriers. The measured electrode voltage (V) is then given by

$$V = \phi_{\rm S} + V_{\rm H} + V_0, \tag{2}$$

where V_0 contains all of the additional, constant potential drops (including the potential drop in the Gouy layer, which is considered to be negligible, as discussed above).

Experimental details

OCP The measurement of the open-circuit potential is performed between a working electrode and a reference electrode at an open circuit at which no (or negligible) current flows through the electrochemical cell during the measurement. In practice this is accomplished by connecting both electrodes through a mV-meter with extremely high input impedance (>10 12 Ω -cm). The mV-meter applied in this work also enables the connection of a temperature probe and acts as the interface to a computer, which samples the potential and the temperature as a function of time (up to several hundreds of measurement points per second). Silicon device wafers

[CZ, 125 and 150 mm, p-type, boron-doped, $16-24 \Omega$ -cm, with (100) surface orientation have been applied as working electrodes, except in Figure 15 (shown later), where only pieces of a p-type, 200-mm wafer were used (total area of sample exposed to liquid was 3 cm²). The wafer was mounted in a specially designed single-wafer holder made of PFA (perfluoroalkoxy copolymer) so that only the polished front side of the wafer (about 95% of the area) was exposed to the electrolyte under investigation. Ohmic contact between the silicon electrode and the wiring was established by sputtering 700 nm of Al on the back side of the p-type wafer, followed by sintering at 435°C for 30 minutes. For the experiment displayed in Figure 15, a different approach, creating the ohmic contact on the back side of the sample with an In/Ga eutectic mixture, was used. To realize a chemically compatible and stable reference potential, several different approaches have been tested. For absolute measurements, a standard Ag/AgCl electrode [3M KCl/sat. AgCl, +204 mV vs. N.H.E. (normal hydrogen electrode) at 20°C] fitted with a PFA capillary salt bridge has been used very successfully in HF, SC1, and aqueous NH, solutions. The leakage rate of this capillary was determined to be less than 200 µl saturated KCl electrolyte per 24 hours. Measurements in this paper which refer to Ag/AgCl are measured relative to this setup with the capillary salt bridge, except for Figure 15, where a gel-filled reference electrode was applied. Other reference systems tested were also based on Ag/AgCl standard reference systems, but their absolute potentials vs. N.H.E. were not determined; measurements involving these systems are referred to an arbitrary reference. These deviations in the reference potential were introduced through additional junctions (glass fiber) and leaking of chemicals into the reference system.

A special reference system has been developed in order to provide contamination-free measurements. In this case, a second Si wafer encapsulated in PFA has been used as the reference electrode. This "reference wafer" is of the same type as the working electrode, with one difference: It is already in a passivated state; i.e., all major surface reactions (oxidation, etching) are completed, resulting in a sufficiently stable reference potential. This stability is achieved by immersion of the reference wafer in the solution at least 20-30 minutes before the actual measurement (depending on the process, longer times may be required). Then the working electrode is immersed, and the potential changes due to the ongoing surface reactions (on the working electrode) are measured vs. the Si reference wafer. In this case, the potential is referred to a Si reference. Under certain circumstances (e.g., when measuring in HF), it is advantageous to use a different wafer type as reference system [e.g., wafers with (111) orientation or different doping] to achieve a more stable

reference potential. Throughout the paper, all chemical concentrations given in percentage are weight % if not stated otherwise. Also, all measurements were performed in open tanks, exposed to clean-room air, so all chemical solutions can be considered as saturated with oxygen.

As is shown in the following discussion, there is a very good correlation between measurement results obtained with this OCP technique and results obtained with well-established surface-characterization techniques. However, the OCP is influenced in a very complex way by several processes occurring simultaneously which are described in summary by only one measurement value at a time, reflecting any changes at the semiconductor/electrolyte interface by a chemical (e.g., oxidation, etching, dissolution) or physical process (e.g., adsorption). By calibrating the OCP responses with well-established surface-characterization techniques, the time-dependent variation of the OCP can be used as a signature for the ongoing surface reactions, leading to a qualitative and eventually quantitative understanding.

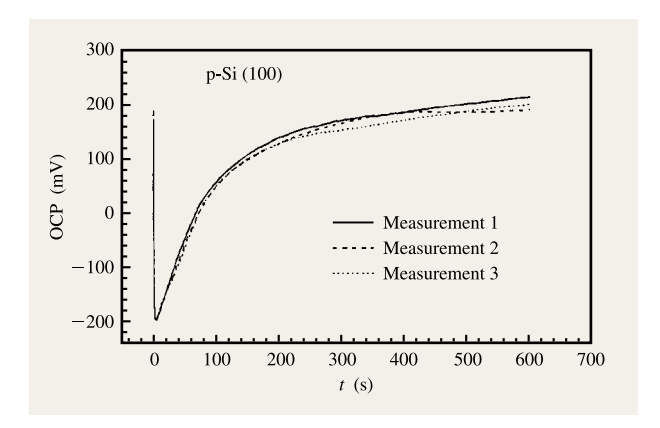
MIR–FTIR Double-side-polished IR samples [p-type, (100) surface orientation, 10–25 Ω-cm] were immersed sequentially in a 0.5% HF mixture after an SPM/DI-rinse pretreatment. At preselected times determined from the OCP curve, the samples were removed from the HF bath and immersed for a maximum of five seconds in DI water and then blow-dried with N₂. The samples were then transferred to a Mattson-galaxy FTIR spectrometer and measured within 20 minutes after preparation with p-polarized light at a resolution of 4 cm⁻¹ in the range from 2030 to 2170 cm⁻¹. All samples were measured with the initial SPM oxide as reference.

SE Si wafers of the same type as used for the OCP measurements (see above) were immersed together with the working electrode in different SPM or SC1 test solutions after an HF/DI-rinse pretreatment. After the SPM or SC1, the wafers were rinsed for ten minutes in DI water and then blow-dried with N_2 . Spectroscopic ellipsometry measurements were performed immediately after sample preparation, using a SOPRA ES4G ellipsometer (photon energy range 2.76–4.86 eV in 21 equidistant points, angle of incidence: 80°). To obtain more accurate $\tan \Psi$, $\cos \Delta$ data, three measurements per wavelength were averaged.

XPS Samples were prepared in the same way as described above for SE and then analyzed, looking at the Si 2p, O 1s, and C 1s lines.

Experimental results and discussion

The experimental results are discussed in order of the simplicity of the chemical reactions occurring on the



Typical time evolution and reproducibility of the OCP of a p-type Si wafer during immersion in an SPM mixture at 95°C (preconditioning: 5 min 0.5% HF, followed by 2 min DI-water rinse). The OCP was measured relative to an arbitrary reference (see experimental section). Reprinted from [46] with permission of the ECS.

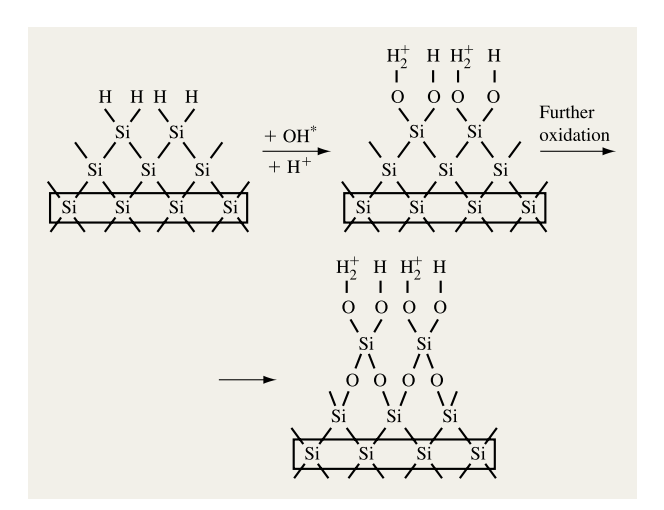


Figure 2

Schematic and simplified representation of the major changes on the silicon (100) surface when immersed after hydrogen passivation in an SPM mixture. Reprinted from [51] with permission of the ECS.

electrode surface. The initial reaction is with the SPM (sulfuric acid/hydrogen peroxide) mixture, which oxidizes the silicon surface. This is followed by measurements in HF (hydrofluoric acid), where two consecutive processes occur: first, the chemical dissolution of SiO₂, followed by electrochemical etching of the last monolayer of Si. The third part of the experimental discussion deals with the

dissolution of SiO₂ in NH₄OH (aqueous ammonia) solutions, where, besides chemical and electrochemical etching of the surface, rate-determining adsorption phenomena are most probably involved. In the final part, we briefly investigate the SC1 mixture (aqueous ammonia/hydrogen peroxide/water), which involves oxidation and dissolution reactions occurring simultaneously.

• Oxidizing environment (SPM)

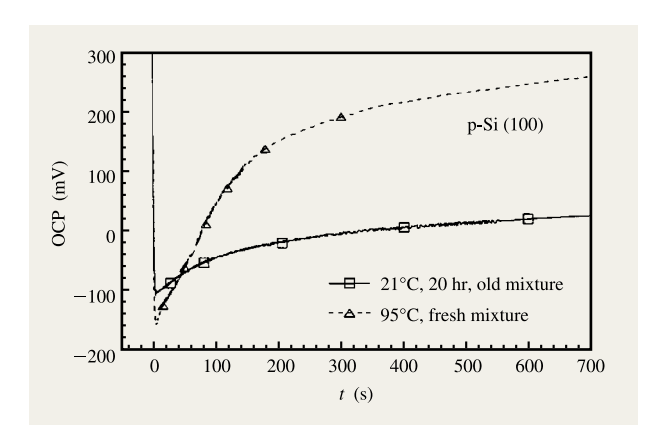
When Si is oxidized, the Si/SiO₂ interface is being displaced step by step from the original Si surface and located deeper within the Si wafer. For this process, the oxidizing species moves through the oxide layer to react with Si at the interface. Since such an oxidation process involves a drastic change in the chemical and physical appearance of the Si surface, a change in the potential distribution at the interface is expected. Figure 1 presents a typical time response of the OCP of a hydrogen-passivated Si surface during immersion in a strongly oxidizing chemical mixture. The results from three identical measurements are presented to demonstrate the high reproducibility of the measurement method.

A very sharp decrease of the potential to more negative values is initially observed, yielding a characteristic minimum potential which in the subsequent discussion is called the point of minimum potential, or PMP. In this initial phase (lasting around four to five seconds), the hydrophobic surface turns into a hydrophilic one by exchanging its surface hydrogen atoms with partly protonated hydroxyl groups, as shown in **Figure 2**. This first step is believed to be an oxidative attack on the hydrogen-passivated silicon by strong oxidizing species existing in this mixture. A free hydroxyl radical is shown as an example; it is an intermediate in the reduction of H_2O_2 , $S_2O_8^{2-}$, and H_2SO_5 (Caro's acid).

After this initial drop, the OCP reverses the direction with a decreasing rate as the oxidation process continues. Further steps involve back-side oxygen insertion, resulting in a wet-chemical oxide of a few monolayers' thickness [52]. It should be noted here that the general appearance of OCP measurement curves is very similar for most of the electrolytes investigated in this work. However, significant differences exist and are discussed as they appear.

Test results for the oxidizing power of an SPM mixture are shown in **Figure 3**. A fresh mixture of sulfuric acid and hydrogen peroxide was prepared and immediately measured with the OCP setup using a hydrogen-passivated silicon wafer as working electrode. The chemical mixture was then allowed to cool down for more than 20 hours before being remeasured with the same procedure. In addition to a lowering of the temperature, most of the hydrogen peroxide in the mixture decomposed. Both

356



Time evolution of the OCP of a p-type Si wafer as a function of the oxidation potential of an SPM mixture. The mixture was aged to reduce the hydrogen peroxide concentration, and its temperature was lowered (preconditioning of the working electrode as in Figure 1). The OCP was measured relative to an arbitrary reference (see experimental section). Reprinted from [51] with permission of the ECS.

changed parameters yielded a chemical solution with strongly reduced oxidation potential. The slope obtained from these curves is the potential change after the PMP and $\Delta_{\rm OCP},$ which is defined as the potential difference between the PMP and the final potential at which a quasisteady state of the oxidation reaction is reached, or the measurement is stopped (i.e., when the sample is removed from the solution).

Investigations made with SE on these two oxides show a small but clear and significant difference in oxide thickness as interpreted from the difference in the refractive index between them and also relative to an H-passivated surface which was also measured. Because of the lack of an appropriate physical model for the oxide layers, real (ϵ_r) and imaginary (ϵ_i) parts of the dielectric functions are calculated assuming that no surface layers are present on the Si substrate; they are then compared with reference data [53] for a bare Si surface to obtain $\Delta \epsilon_r$ and $\Delta \epsilon_i$ (pseudodielectric functions, **Figure 4**). By using this approach, the small difference between the two thin oxide layers is strongly amplified. Additional XPS investigations on these two different oxides (**Figure 5**) confirmed the findings with SE.

These investigations suggest that the slope of the potential change after the PMP and the absolute difference between the PMP and the final potential ($\Delta_{\rm OCP}$) can be correlated respectively to the oxidation rate and the resulting oxide thickness. **Table 1** lists values for the oxide thickness calculated from SE and XPS data by applying models used for very thin (2–3 nm) thermal

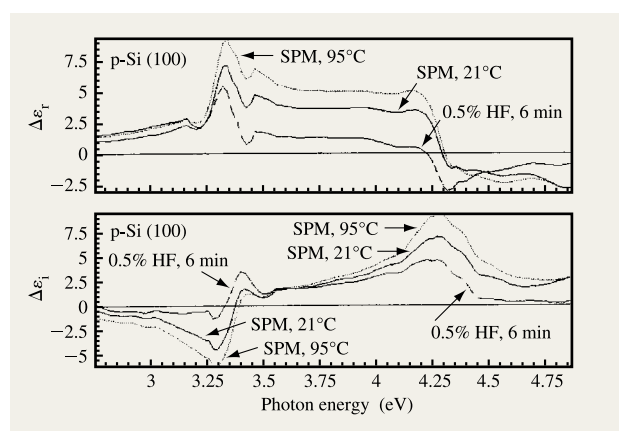


Figure 4

Real $(\Delta \varepsilon_r)$ and imaginary $(\Delta \varepsilon_i)$ parts of pseudodielectric functions, plotted vs. photon energy for p-type Si wafers treated in different mixtures (Figure 3). Reprinted from [46] with permission of the ECS.

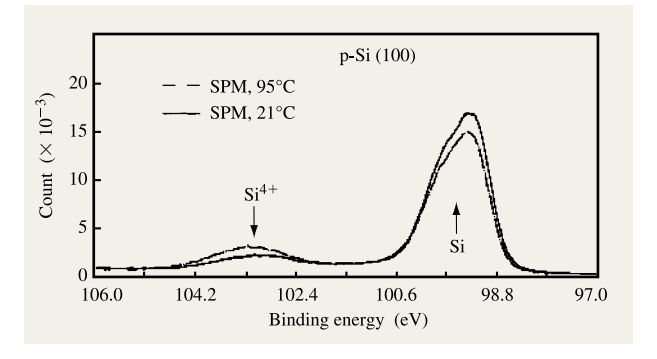


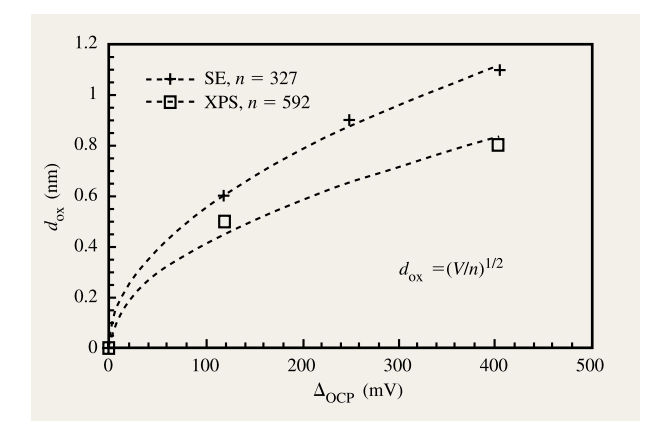
Figure 5

XPS spectra for p-type Si samples treated in different SPM mixtures (Figure 3). Reprinted from [47] with permission of the ECS.

Table 1 Calculated oxide thickness from XPS (d_{XPS}) and spectroscopic ellipsometry (d_{SE}) measurements and correlation to the potential difference between the PMP and the potential after 600 s immersion time (Δ_{CCP}) .

Sample treatment	$d_{ ext{XPS}}$ (nm)	$d_{\mathrm{SE}} \pmod{\mathrm{nm}}$	$rac{\Delta_{ m OCP}}{({ m mV})}$
SPM, 21°C	0.5	0.6	120
SPM, 75°C	_	0.9	250
SPM, 95°C	0.8	1.1	405

oxides. An additional measurement was carried out with an SPM mixture at 75°C. The difference in the oxide thickness between SE and XPS is related to the models



Correlation between $\Delta_{\rm OCP}$ (potential difference between the PMP and the potential after 600 s immersion time) and oxide thickness calculated from SE and XPS measurements (see Table 1). Reprinted from [51] with permission of the ECS.

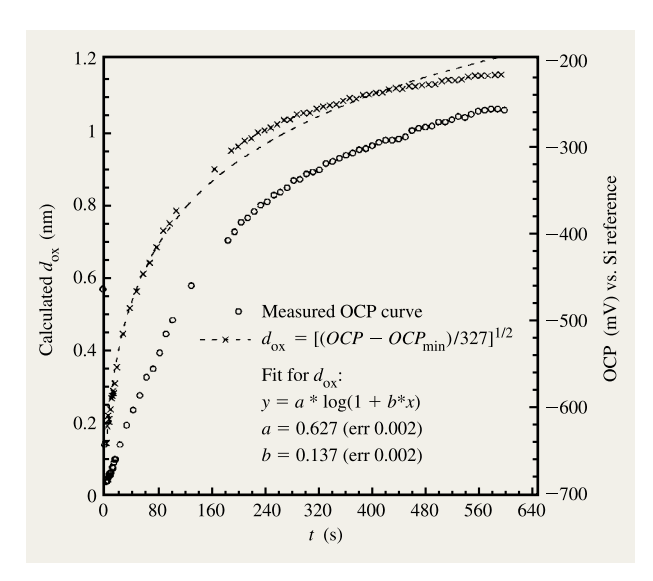


Figure 7

Oxide thickness (d_{ox}) as a function of time, calculated from an OCP curve which was measured when a p-type wafer was immersed in a 102°C SPM mixture (pretreatment as in Figure 1). Reprinted from [51] with permission of the ECS.

applied for the calculations. For further calculations, the values calculated from SE measurements are used.

Figure 6 shows the correlation between $\Delta_{\rm OCP}$ and oxide thickness, calculated from SE and XPS measurements. Assuming an additional point at $d_{ox} = 0$ when $\Delta_{OCP} = 0$, a parabolic dependence of the potential on the oxide

thickness was found, confirming the theoretical findings [48]. In this theoretical approach, assuming that the semiconductor surface is depleted during the whole oxidation process, the Poisson equations for the system electrolyte/SiO₂/Si have been solved. Also, $\phi_{\rm H}$ was assumed to be constant during the whole oxidation

The general form of the obtained relationship between the measured potential difference (Δ_{OCP}) and the resulting oxide thickness (d_{ox}) is given by

$$V = m + (p + o)d_{ox} + nd_{ox}^{2}, (3)$$

with

$$m = \frac{qQ_{\text{ox}}^2}{2N_{\text{sub}}\varepsilon_{\text{Si}}}, p = \frac{qQ_{\text{ox}}N_{\text{ox}}}{2N_{\text{sub}}\varepsilon_{\text{Si}}}, o = \frac{qQ_{\text{ox}}}{\varepsilon_{\text{ox}}}, n = \frac{qN_{\text{ox}}^2}{8N_{\text{sub}}\varepsilon_{\text{Si}}},$$
(4)

where V is the measured $\Delta_{\rm OCP}$ (V); q (electronic charge) = 1.6022×10^{-19} C; $\varepsilon_{\rm ox}$ (dielectric constant for thermal oxide) = 0.34×10^{-19} F-nm $^{-1}$; $\varepsilon_{\rm Si}$ (dielectric constant for Si) = 1.05×10^{-19} F-nm⁻¹; N_{sub} (doping level of the Si substrate, equivalent to a boron-doping level of 7×10^{14} cm⁻³) = $6.5 \times 10^{-7} \text{ nm}^{-3}$; N_{ox} = charge in the oxide (nm⁻³); and $Q_{\rm ox}$ (charge on the oxide surface¹) = $4.92 \times 10^{-6} \, \rm nm^{-2}$. By fitting this function to the experimental results displayed in Figure 6, with $N_{\rm ox}$ as fitting parameter and calculating the single terms, it can easily be seen that the terms m, p, and o are negligibly small, resulting in a simplification of the equation to

$$V = nd_{\text{ox}}^2, \tag{5}$$

and yields: $N_{\rm ox} = 1.06 \times 10^{-3} \text{ nm}^{-3}$ (i.e., $1.06 \times 10^{18} \text{ cm}^{-3}$). This value is in very good agreement with literature data for wet-chemical oxides (grown in acid mixtures) ranging from 2×10^{11} cm⁻² to 6×10^{12} cm⁻², where the oxide charge density has been determined with a surfacecharge analyzer² [54].

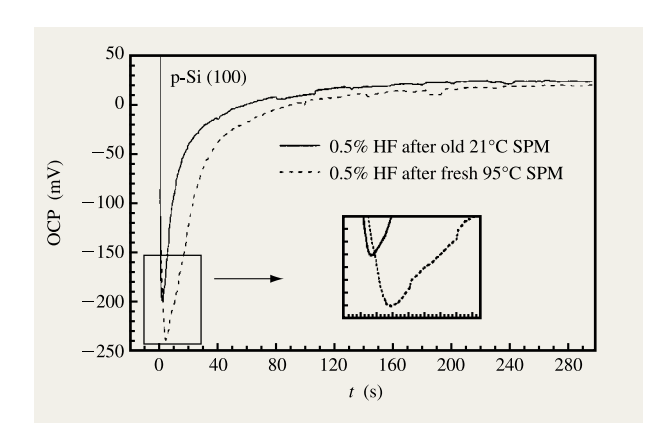
With this correlation between oxide thickness and potential change, it is now possible to calculate $d_{--}(t)$ for an OCP(t) curve, which is shown in Figure 7 (by using the results from SE measurements). In the beginning, the calculated $d_{ox}(t)$ follows (with relatively good agreement) the logarithmic law which was proposed for the oxidation process of several metals [55] and silicon [56] at elevated temperatures:

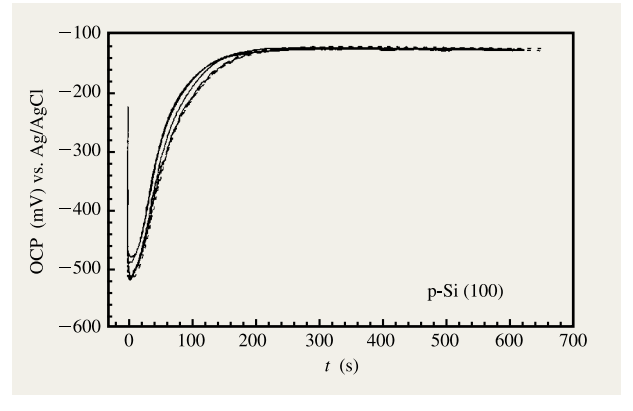
$$d_{ox} = k \log(1 + bt), \tag{6}$$

where d_{ox} is the oxide growth in time t, and k and b are constants.

 $^{^{1}}$ $Q_{\rm ox}$ can be calculated assuming that all positive charge on the oxide surface originates, depending on the pH of the electrolyte, from protonated surface silanol groups (Si–OH₂⁺); see [48].

² P. Snee, Motorola, East Kilbride, UK, private communication.





Shift of the OCP curve to longer etch times and lower PMP with the thickness of wet-chemical oxides (preconditioning as in Figure 3). The OCP was measured relative to an arbitrary reference (see experimental section). Reprinted from [47] with permission of the ECS.

Figure 9

Typical time evolution and reproducibility of the OCP of a p-type Si wafer when immersed in a 0.25% HF solution under clean-room light conditions (preconditioning of the electrode by wet-chemical oxidation with SC1, 0.25/1/5, 10 min at 70°C, followed by 10 min DI-water rinse). Reprinted from [47] with permission of the ECS.

• Acid-etching environment (HF)

Another way to estimate the relative difference in the thickness of native oxides on semiconductors is to monitor the OCP as a function of time while dissolving the oxide in an appropriate medium, e.g., HF. Figure 8 presents the results obtained when the two different oxides under investigation (see Figure 3) are etched off in 0.5% HF. The PMP is found to be the point which marks the time at which the major part of the oxide is chemically dissolved and another process (electrochemical etching) begins to determine the potential change (see discussion below). By assuming that the oxide dissolution time changes linearly with the oxide thickness, a shift of the PMP by a factor of 2 would be expected from the SE and XPS measurements given above, which indeed was observed. The sensitivity of this technique for determining relative differences in the oxide thickness by comparing the time required for various samples to reach the PMP can be strongly increased by using lower HF concentrations, as is later demonstrated.

Figure 9 presents the typical time evolution of the OCP of a p-type Si substrate immersed in a 0.25% HF solution after SC1 oxidation and DI rinse. The measurement was performed under clean-room light conditions. The initial OCP value was difficult to quantify because of the finite time needed for immersion of the working electrode (0.5 to 1 s), but was found in general to be near the final steady-state potential (and, in many cases, higher). In the initial stage of the reaction, the native oxide layer is dissolved, resulting in a drift of the OCP to more negative values [57]. After reaching a characteristic minimum (the PMP), which is defined by several parameters

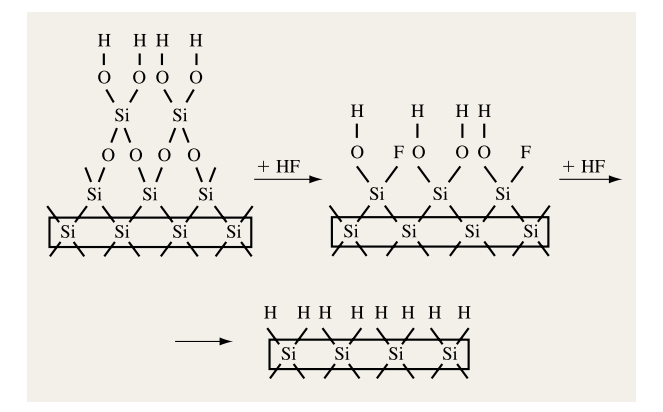
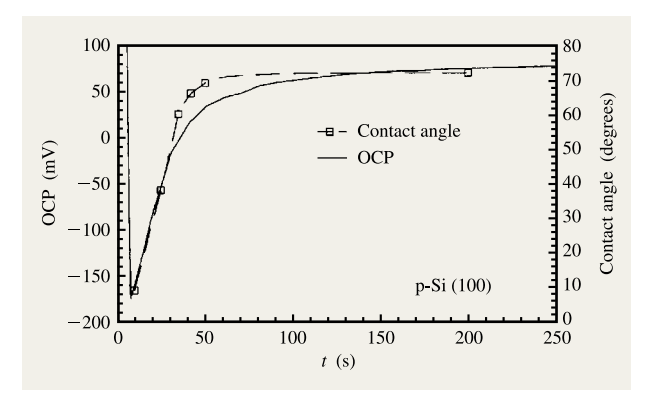


Figure 10

Schematic and simplified two-dimensional representation of the major changes on the silicon (100) surface when immersed in an oxidized state in an HF solution. Reprinted from [47] with permission of the ECS.

(e.g., thickness of the oxide, etch speed, pH of the mixture, illumination), the OCP reverses direction until it reaches a quasi-steady-state potential. Here no further major surface changes occur, except for a slow chemical corrosion of Si. This results in a slow increase of the potential with time depending on illumination and wafer doping [48]. Figure 9 also displays the reproducibility of OCP measurements in HF (HF mixture in an open tank prepared freshly every day). The same pretreatment and measurement



Correlation between the time evolution of the OCP and the contact angle of a p-type Si wafer in a 0.5% HF solution (clean-room light conditions; preconditioning: SPM, 10 min at 95°C, followed by 10 min DI-water rinse). The OCP was measured relative to an arbitrary reference (see experimental section). Reprinted from [51] with permission of the ECS.

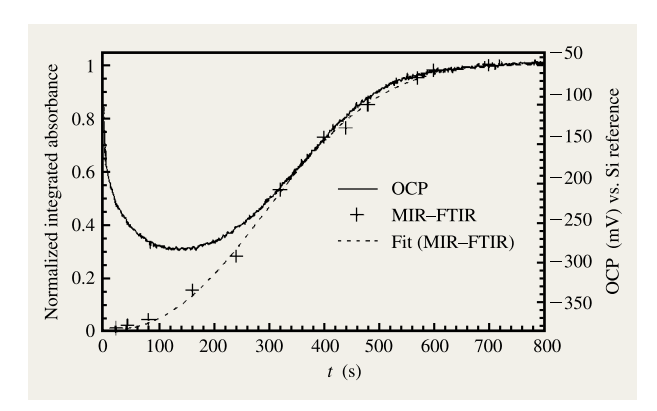


Figure 12

Correlation between the time evolution of the OCP of a p-type Si wafer when immersed in a 0.1% HF solution and the corresponding normalized integrated absorbance calculated from MIR–FTIR measurements (measured vs. a hydrogen-passivated Si wafer of the same type as the reference electrode under clean-room light conditions; sample preconditioning: SPM, 10 min at 101°C, followed by 10 min DI-water rinse). Reprinted from [51] with permission of the ECS.

procedure was performed six times on three different days with two different Si electrodes of the same type.

Figure 10 again shows a very schematic and simplified representation of the major changes on the silicon (100) surface when immersed in an oxidized state in an HF solution. In the first step, the wet-chemical oxide is dissolved by HF molecules, forming SiF_6^{F} ions in solution,

which results in a fast drop of the potential to more negative values. The second major step is the etching of the last monolayer of Si²⁺, which is bonded to the bulk material. As a result of this process, the potential again shifts to more positive values. Finally, a relatively constant potential is reached, indicating that a nearly complete hydrogen passivation of the silicon surface has been obtained. This final potential is a mixed potential, or so-called corrosion potential, which is determined by the anodic and cathodic processes occurring at the interface. Correlation with contact-angle measurements (Figure 11) and MIR-FTIR (Figure 12) shows that the quasi-steady-state potential indicates the relative completion of the hydrogen surface passivation layer. Recent work exploring these cathodic and anodic processes partially by using open-circuit potential measurements has been reported by L. Torcheux et al. [58] and V. Bertagna et al. [59, 60]. In these studies, the electrochemical properties and reaction kinetics at the mono- and polycrystalline silicon surfaces in HF solutions as a function of exposure to light, doping type, dopant concentration, oxygen content in the electrolyte, and deposition conditions for the polycrystalline material have been investigated. The phenomenon of electroless plating of Cu contamination onto the silicon surface from HF solutions is also discussed.

Figure 12 shows an OCP curve of a p-type Si wafer immersed in a 0.1% HF solution under clean-room light conditions. The measurement was performed vs. a hydrogen-passivated Si wafer of the same type as the working electrode. After the OCP measurement, appropriate times for the treatment of IR samples were chosen from the curve. The preconditioning for the electrode as well as for the IR samples was an SPM oxidation, ten minutes at 101°C, followed by a ten-minute DI-water rinse. The integrated absorbance has been normalized under the assumption that a 99% coverage of the surface with Si–H_x groups is eventually reached, which is in agreement with measurement results obtained by Gräf et al. [61].

Figure 12 shows that the etching of the last monolayer of oxidized Si occurs slowly before the PMP and yields $\sim 10\%$ coverage of the surface by Si- H_x groups at the PMP. This electrochemical etching of the surface influences the OCP curve and appears to become the only dominating surface reaction after ~ 350 s, where the IR and the OCP curves match. This finding was confirmed by XPS measurements [48]. The fit of the MIR-FTIR data (integrated absorbance) was performed using the so-called Johnson-Mehl equation [62], which is a general empirical equation for a quantitative description of overall transformation kinetics:

$$X = 1 - \exp[-(kt)^f],$$
 (7)

360

where X is the volume fraction transformed, k the reaction-rate constant (t^{-1}) and f the time exponent (dimensionless). Originally developed for nucleation and growth processes of layers on a solid surface, this theory shows good applicability for the problem described here, where one monolayer must be removed.

Figure 13 presents the results of an experiment in which the etching of equal wet-chemical oxides (SPM/DI rinse) and the buildup of H passivation as a function of the HF concentration (i.e., total fluorine concentration) were studied. A significant change in the slope of the OCP before and after the PMP was obtained, resulting in a major time delay in reaching the final surface passivation with a reduced HF concentration. Recently Chyan et al. [63] were not able to reproduce these typical OCP curves, which are obtained when etching silicon oxides in HF [46, 47]. Instead, when immersing a "thin native oxide" in 0.01% HF, they observed only the initial potential drop, which took ~150-200 min to reach a value close to the PMP. To explain these rather strange findings, it is possible that their HF concentration was even lower than the reported 0.01%. This would extend the etching process to very long times or render it impossible to reach H passivation. They also reported that the sample surface after the measurement was highly hydrophobic and hydrogen-terminated (measured respectively by contact angle and infrared absorption). Instead of H termination, the hydrophobicity of the sample might indicate that the etching process was disturbed by heavy organic contamination on the surface. However, it is difficult to explain their IR absorption findings, as well as their baseline potential for the HF-etched silicon sample (in 0.49% HF) without further details.

It has been shown (Figure 8) that the OCP technique is very sensitive for determining small differences in the thickness of native oxides. Figure 14 presents another instance in which small chemical differences of the surface were investigated. Initially the electrode was passivated in a 0.5% HF solution. In the first case ("HF after HF"), the electrode was removed from the bath and immediately immersed again. In the second case, the electrode was removed from the HF solution and rinsed in DI water for ten minutes and then immersed again in the HF bath. While the HF-treated surface immediately returned to the initial quasi-constant potential, the DI-rinsed sample required 30-40 s to achieve the steady state. The difference is small but again significant, and is believed to be due to the reoxidation of the silicon surface in the DI water, which was also observed by Gräf et al. [61].

Very recent work in this field carried out at IBM demonstrates that the OCP technique can also be applied for the investigation of the etching behavior of thermally grown or deposited dielectric materials. An example is given in **Figure 15**, which represents the etching process

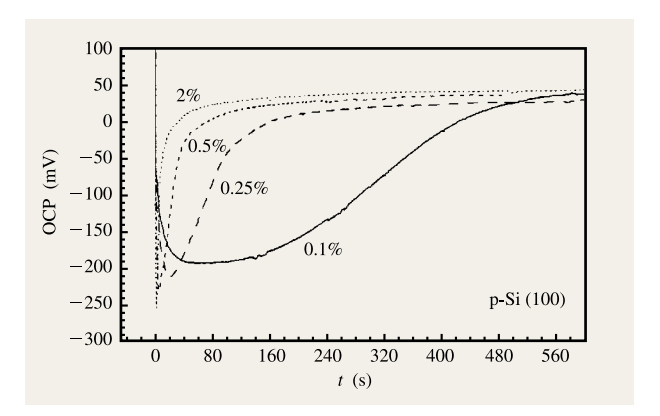


Figure 13

Time evolution of the OCP as a function of the HF concentration (preconditioning: SPM, 10 min at 101°C, followed by 10 min DI-water rinse). The OCP was measured relative to an arbitrary reference (see experimental section). Reprinted from [46] with permission of the ECS.

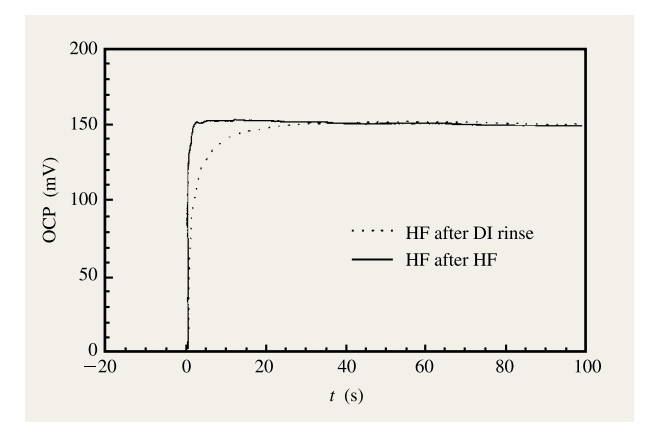
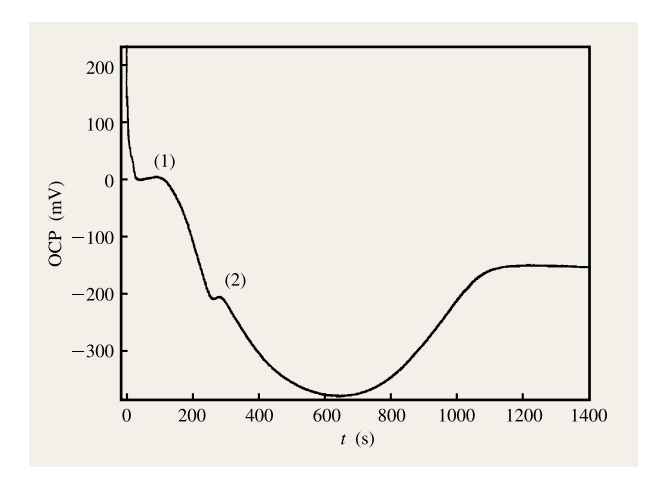


Figure 14

OCP curves for a p-type Si electrode immersed in a 0.5% HF bath after a 10 min DI rinse ("HF after DI rinse") and just after removal from the HF bath ("HF after HF"). The OCP was measured relative to an arbitrary reference (see experimental section).

of a 2.5-nm oxide (O₂, 700°C, 8 min, as measured by ellipsometry) when immersed in a 0.1% HF solution. In general, the OCP response measured during the etching of a thermally grown oxide is very similar to that observed with native oxides. However, there are some significant differences, the first being a delay in the initial potential drop (1) about 32 s after immersion of the sample in the HF. A possible explanation for this behavior is that an etch barrier is reached within the oxide. This is believed to be the interface between the annealed chemical oxide



OCP response over time for the etching process of a 2.5-nm thermal oxide layer (O_2 , 700°C, 8 min) on p-type silicon, when immersed in a 0.1% HF solution.

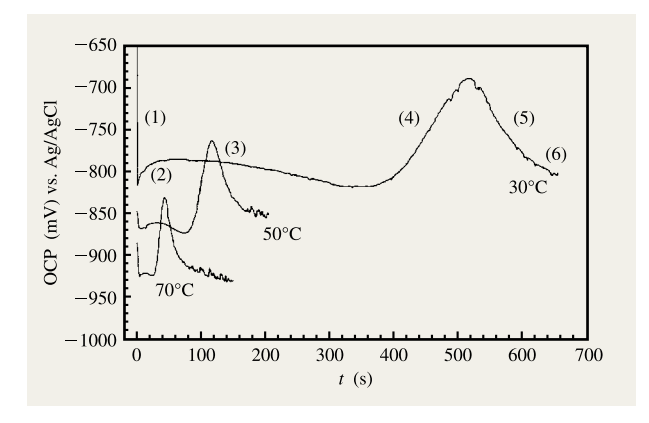


Figure 16

OCP curves for the dissolution of SiO_2 in NH_4OH as a function of temperature (pretreatment: 0.25/1/5 SC1, 10 min at room temperature followed by DI-water rinse).

("residue" from the hydrophilic-last cleaning before the oxidation process) and the thermally grown part of the dielectric layer. The second difference is observed in the lower part of the curve at $\sim\!260$ s after immersion of the sample (2). This deviation of the potential is believed to signal the initial breakthrough of the HF to the bare silicon and the initial accumulation of H-terminated silicon bonds (discussed earlier). The appearance of this second potential deviation gives an indication of the uniformity of the etching process, since the main potential change is still determined by the dissolution of the silicon

dioxide until the PMP is reached. In cases (1) and (2), the surface re-establishes a new surface charge, which causes an adjustment of the carrier distribution in the space-charge layer of the semiconductor.

• Caustic etching environment (aqueous solution of NH₂) Another medium in which SiO₂ dissolves is an aqueous solution of ammonia (NH₂). It is a component of the SC1 mixture, where it has the role of slowly dissolving the formed oxide in order to under-etch particles and by doing so remove them from the substrate surface. Under conditions in which the dissolution reaction is faster than the oxidation of the Si by H₂O₂, OH⁻ attacks the surface and causes surface roughening. To evaluate the speed of the dissolution reaction, several OCP measurements have been performed. The electrode was preoxidized with a 0.25:1:5 SC1 mixture (volume ratios NH₄OH/H₂O₂/H₂O) at room temperature for ten minutes. Then the electrode was rinsed for ten minutes in DI water and subsequently immersed in an NH₄OH (30%)/H₂O mixture (0.25:6 volume ratio, i.e., $\sim 1.4 \text{ mol-l}^{-1} \text{ NH}_3 \cdot \text{H}_2\text{O})$ at different temperatures. The results are displayed in Figure 16.

The responses obtained are very different from those of OCP curves discussed to this point, but they are again highly significant and reproducible. In the initial phase (1), the potential drops rapidly to a minimum. After that the potential increases (2) until it reaches a certain maximum. In the next part of the curve (3), the potential again drops back to more negative values, close to the initial PMP. After it has reached a minimum, the OCP increases again (4) to more positive values until it decays (5) to a more negative value, where the Si corrodes very heavily under H₂ gas evolution (6). A possible explanation for this very interesting behavior is as follows. In part (2) of the curve, adsorption of NH₃ and/or NH₄ molecules takes place on the negatively charged silica surface. As has been reported [19, p. 317], this process reduces the rate of dissolution of silica. When a certain coverage is attained, where the formation of surface complexes increasingly weakens the Si-O back bonds, dissolution can proceed [20, p. 175]. Once the dissolution process is initiated, it proceeds at a rate that is strongly dependent on the temperature until all of the SiO₂ is dissolved (3). This is demonstrated with measurements at different temperatures. The next step is similar to what has been observed in HF solutions, in which the last monolayer of Si^{n+} (n = 1, 2, 3) must be etched electrochemically (4) with a possible buildup of an over-voltage to activate the Si back bonds for the further etching reaction. Once the maximum is reached, the potential moves (5) toward the corrosion potential for Si in NH₄OH (6). H, gas-bubble evolution from the Si surface happens about halfway after the maximum along the curve (5). It has also been observed that the electrode

surface remains hydrophilic until about halfway between (5) and (6).

• Oxidizing and etching environment (SC1)

The last mixture discussed here is the SC1 solution, which is the most complicated chemical mixture to be analyzed with the OCP technique because two overall reactions occur simultaneously. The first is the oxidation of Si to SiO₂ by H_2O_2/HO_2^- , and the second the OH⁻-catalyzed dissolution of SiO, by H,O. In a first experiment, the temperature dependence of the reactions at a p-type Si surface was studied. The results are presented in Figure 17. While the room-temperature measurement rapidly reaches a quasi-constant potential, it takes considerable time for the 70°C experiment to do so. This might be explained by the increased dissolution rate of the oxide compared to the low-temperature process. The consequence is that a much longer time is needed to find a condition of equilibrium between the processes—the dissolution of the oxide on the oxide/electrolyte interface and the continuous oxidation process at the oxide/silicon interface. The relative difference in the oxide thickness between the samples after the SC1 treatment at the two temperatures has been determined by OCP measurements in 0.25% HF, resulting in a small difference of the responses. It appears that the sample after the hightemperature SC1 treatment achieves a lower PMP and reaches H passivation a little faster [48]. Additional XPS investigations revealed no significant difference between the two oxides. However, SE studies showed a small but significant and reproducible difference [48]. It can be speculated that the high-temperature process causes more etching of the surface. Especially at the beginning, the etching process appears dominant; thus, a higher degree of surface roughness could be the reason for the small differences observed.

Another question which frequently arises is whether sonic agitation of the chemical mixture influences the surface reaction. To evaluate this, a Si electrode was immersed in a circulated SC1 tank at room temperature once with and once without sonic agitation (300 W, 854 kHz). Since the results showed no significant difference between the OCP responses, it can be concluded that sonic agitation does not influence the surface reaction.

Interesting observations have recently been made by using the OCP technique to investigate metal adsorption from SC1 mixtures onto the silica surface [64, 65]. In these reports it has been demonstrated that the OCP technique can also be used as a very sensitive monitoring technique for low levels of metal contamination in chemical cleaning mixtures. As discussed earlier in this paper, metal ions or their aqua- or hydroxo-complexes can adsorb onto the silica surface and so change the surface potential, i.e., the charge residing on the surface. This

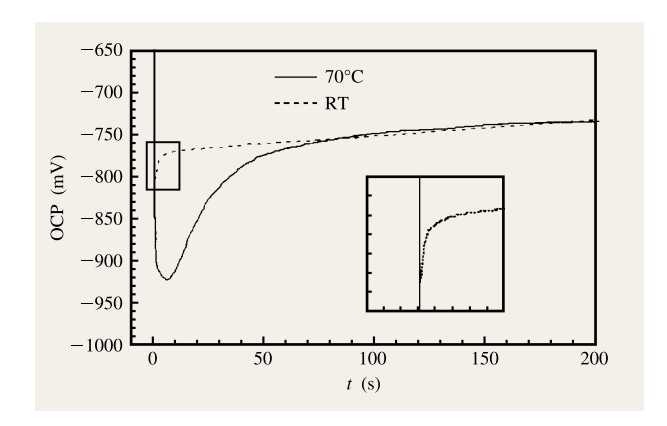


Figure 17

OCP curves for a p-type substrate immersed in a hydrophobic state in an SC1 mixture at different temperatures (0.25/1/5, pretreatment: 0.5% HF, 5 min followed by 4 min DI-water rinse). The OCP was measured relative to an arbitrary reference (see experimental section).

change causes a redistribution of charge carriers in the space-charge layer of the semiconductor and therefore can be measured quantitatively by monitoring the open-circuit potential.

Summary

The rapid approach of advanced gate dielectrics and increasing interest in high-k materials raise new challenges for the cleaning community. The influence of native oxides on the final dielectric property of the gate material must be better understood, and significant research work is still necessary to develop and optimize adequate cleaning processes. In this paper, a technique based on OCP measurements is a promising candidate as an efficient and simple characterization tool for this task which has the capability to deliver the necessary information. It has been demonstrated that this technique provides information about the evolution of semiconductor surface reactions in wet-chemical environments and enables the study of the kinetics of oxidation, dissolution, and etching processes in situ and in real time. OCP results presented in this paper are in good agreement with results obtained from MIR-FTIR, XPS, SE, and contact-angle studies, and demonstrate very good repeatability and high sensitivity. A model was also developed which makes it possible to obtain quantitative information on the thickness of a growing native oxide at any time. With this model it is possible to study the kinetics of wet-chemical oxidation processes on semiconductor surfaces (a very difficult and time-consuming process until now), as well as the dissolution and etching behavior of semiconductor

oxides and substrates [13]. It has also been shown for the first time that the OCP technique can be applied for the investigation of thermally grown oxides. Initial results yielded unique information on the structural composition of an ultrathin dielectric layer and the uniformity of the etching process.

Acknowledgments

The author thanks Marc Heyns and the Ultra Clean Processing group, and many others at IMEC, Leuven, Belgium, for their friendship of many years and their support for the major part of the work reported in this paper. Except for the experiment described in Figure 15, all experimental work was performed at IMEC, Leuven, Belgium, by the author between 1992 and 1995. Special thanks go to Serge Biesemans (currently at IBM Microelectronics, East Fishkill, New York) and Ivo Teerlinck for many critical discussions and contributions to the understanding of OCP measurements; and to Hugo Bender, Wolfgang Storm (currently at Wacker Siltronic, Burghausen, Germany), Diana Tonova (University of Sofia, Bulgaria), and Patricia Van Marcke for performing the MIR-FTIR, XPS, and SE measurements, respectively. Geert Doumen and Bert Vermeire (currently at the University of Arizona) are acknowledged for their assistance in adjusting software and hardware problems for the measurement setup. The author thanks the students Werner Poot (KU Leuven, Belgium), Joost van Raaij (TU Eindhoven, Netherlands), Dimitrios Vassilakopoulos (NTU Athens, Greece), Felix Muniz Espada (University of Valladolid, Spain), and Athina Kokkinidou (University of Thessaloniki, Greece) for the experimental support during their summer internships. The author also thanks David L. Rath and Henry Grabarz for their support in establishing a reliable experimental setup, and Patrick Varekamp for providing the ultrathin oxide samples for the portion of the work performed at IBM.

References

- Symposium on Cleaning of Electronic Device Components and Materials, Vol. 246, American Society for Testing and Materials, Philadelphia, 1958.
- Handbook of Semiconductor Wafer Cleaning Technology,
 W. Kern, Ed., Noyes Publications, Park Ridge, NJ, 1993.
- 3. W. Kern and D. A. Puotinen, RCA Rev. 31, 187 (1970).
- M. Meuris, P. M. Mertens, A. Opdebeeck, H. F. Schmidt, M. Depas, M. M. Heyns, and A. Philipossian, *Solid State Technol.* 38, 109 (1995).
- T. Hattori, T. Osaka, A. Okamoto, K. Saga, and H. Kuniyasu, J. Electrochem. Soc. 145, 3278 (1998).
- 6. T. Ohmi, J. Electrochem. Soc. 143, 2957 (1996).
- J. Ruzyllo, in Handbook of Semiconductor Wafer Cleaning Technology, W. Kern, Ed., Noyes Publications, Park Ridge, NJ, 1993, p. 201.
- 8. H. Luo and C. E. D. Chidsey, *Appl. Phys. Lett.* **72**, 477 (1998).

- P. L. Cowan, J. A. Golovchenko, and M. F. Robbins, *Phys. Rev. Lett.* 44, 1680 (1980).
- J. R. Patel, J. A. Golovchenko, P. E. Freeland, and H.-J. Gossman, *Phys. Rev. B* 36, 7715 (1987).
- H. M'Saad, J. Michel, J. J. Lappe, and L. C. Kimerling, J. Electron. Mater. 23, 487 (1994).
- H. M'Saad, J. Michel, A. Reddy, and L. C. Kimerling, J. Electrochem. Soc. 142, 2833 (1994).
- G. S. Higashi and Y. J. Chabal, in *Handbook of Semiconductor Wafer Cleaning Technology*, W. Kern, Ed., Noyes Publications, Park Ridge, NJ, 1993, p. 433.
- E. Yablonovitch and T. J. Gmitter, *Diagnostic Techniques for Semiconductor Materials and Devices*, T. J. Shaffer and D. K. Schroeder, Eds., 88-20, The Electrochemical Society, Pennington, NJ, 1988, p. 207.
- M. Takeda, T. Ohwaki, H. Fujii, E. Kusumoto, Y. Kaihara, Y. Takai, and R. Shimizu, *Jpn. J. Appl. Phys.* 37, 397 (1998).
- 16. N. Awaij, Y. Sugita, S. Ohkubo, T. Nakanishi, K. Takasaki, and S. Komiya, *Jpn. J. Appl. Phys.* **34**, L1013 (1995).
- M. Morita, in *Ultra Clean Surface Processing of Silicon Wafers*, T. Hattori, Ed., Springer-Verlag, New York, 1998, p. 543.
- Y. J. Chabal, M. K. Weldon, A. B. Gurevich, and S. B. Christman, *Solid State Phenom.* 65-66, 253 (1999).
- 19. R. K. Iler, *The Chemistry of Silica*, John Wiley & Sons, Inc., New York, 1979.
- 20. W. Stumm, *Chemistry of the Solid Water Interface*, John Wiley & Sons, Inc., New York, 1992.
- 21. P. W. Schindler, B. Fürst, R. Dick, and P. U. Wolf, J. Colloid & Interface Sci. 55, 469 (1976).
- L. M. Loewenstein and P. W. Mertens, J. Electrochem. Soc. 145, 2841 (1998).
- T. Q. Hurd, H. F. Schmidt, A. L. P. Rotondaro, P. W. Mertens, L. H. Hall, and M. M. Heyns, *Proceedings of the 4th International Symposium on Cleaning Technology in Semiconductor Device Manufacturing*, The Electrochemical Society, Pennington, NJ, 1996, p. 277.
- 24. K. H. Beckmann, Surf. Sci. 3, 314 (1965).
- N. J. Harrick and K. H. Beckmann, in *Characterisation of Solid Surfaces*, P. F. Kane and G. B. Larrabee, Eds., Plenum Press, New York, 1974, p. 243.
- H. Ubara, T. Imura, and A. Hiraki, Solid State Commun. 50, 673 (1984).
- E. Yablonovich, D. L. Allara, C. C. Chang, T. Gmitter, and T. B. Bright, *Phys. Rev. Lett.* 57, 249 (1986).
- F. J. Grunthaner and P. J. Grunthaner, *Mater. Sci. Rep.* 1, 65 (1986).
- 29. M. Grundner and H. Jacob, Appl. Phys. A 39, 73 (1986).
- 30. G. W. Trucks, K. Raghavachari, G. S. Higashi, and Y. J. Chabal, *Phys. Rev. Lett.* **65**, 504 (1990).
- 31. H. Gerischer, P. Allongue, and V. Costa Kieling, Ber. Bunsenges. Phys. Chem. 97, 753 (1993).
- W. Storm, W. Vandervorst, J. Alay, M. Meuris,
 A. Opdebeeck, M. M. Heyns, C. Polleunis, and P. Bertrand, Proceedings of the 2nd International Symposium on Ultra Clean Processing of Silicon Surfaces, M. Heyns,
 M. Meuris, and P. Mertens, Eds., Acco, Leuven, Belgium, 1994, p. 367.
- 33. K. Saga and T. Hattori, *J. Electrochem. Soc.* **144**, L250 (1997).
- 34. K. Saga and T. Hattori, *J. Electrochem. Soc.* **143**, 3279 (1996).
- 35. I. Teerlinck, P. W. Mertens, H. F. Schmidt, M. Meuris, and M. M. Heyns, *J. Electrochem. Soc.* **143**, 3323 (1996).
- 36. V. Bertagna, F. Rouelle, G. Revel, and M. Chemla, J. Electrochem. Soc. 144, 4175 (1997).
- 37. T. Homma, C. P. Wade, and C. E. D. Chidsey, *J. Phys. Chem. B* **102**, 7919 (1998).

- 38. I. Teerlinck, P. W. Mertens, M. Meuris, and M. M. Heyns, Proceedings of the Symposium on VLSI Technology, Digest of Technical Papers, IEEE, Piscataway, NJ, 1996,
- 39. H. Kanaya, K. Usuda, and K. Yamada, Appl. Phys. Lett. **67**, 682 (1995).
- 40. K. Wolke, B. Eitel, M. Schenkl, S. Rummelin, and R. Schild, Solid State Technol. 39, 87 (1996).
- 41. G. W. Gale, W. A. Syverson, and J. A. Brigante, Proceedings of the 5th International Symposium on Cleaning Technology in Semiconductor Device Manufacturing, 97-35, The Electrochemical Society, Pennington, NJ, 1998, p. 31. 42. M. Hirose, M. Hiroshima, T. Yasaka, and S. Miyazaki,
- J. Vac. Sci. Technol. A 12, 1864 (1994).
- 43. M. Depas, A. Crossley, B. Vermeire, P. W. Mertens, C. J. Sofield, and M. M. Heyns, presented at the 26th IEEE Semiconductor Interface Specialists Conference, Charleston, SC, 1995.
- 44. M. Houssa, T. Nigam, P. W. Mertens, and M. M. Heyns, Solid State Phenom. 65-66, 249 (1999)
- 45. M. Depas, T. Nigam, K. Kenis, M. M. Heyns, H. Sprey, and R. Wilhelm, Proceedings of the 3rd International Symposium on Ultra Clean Processing of Silicon Surfaces, M. Heyns, M. Meuris, and P. Mertens, Eds., Acco, Leuven, Belgium, 1996, p. 291.
- 46. H. F. Schmidt, I. Teerlinck, M. Meuris, P. W. Mertens, and M. M. Heyns, Proceedings of ALTECH 95, B. O. Kolbesen, C. Claeys, and P. Stallhofer, Eds., 95-30, The Electrochemical Society, Pennington, NJ, 1995, p. 316.
- 47. H. F. Schmidt, I. Teerlinck, W. Storm, H. Bender, M. Meuris, P. W. Mertens, and M. M. Heyns, Proceedings of the 4th International Symposium on Cleaning Technology in Semiconductor Device Manufacturing, The Electrochemical Society, Pennington, NJ, 1996, p. 480.
- 48. H. F. Okorn-Schmidt, "Investigation of Physico-Chemical Mechanisms at the Silicon/Electrolyte Interface Related to Semiconductor Cleaning Technology," doctoral dissertation, Graz University of Technology, Graz, Austria, 1996.
- 49. H. F. Schmidt, M. Hüttinger, and E. Demm, "Application of Electrochemical Techniques for the Investigation of Wet Chemical Etching Processes in Semiconductor Technology," presented at the NATO Advanced Study Institute Symposium on Crucial Issues in Semiconductor Materials and Processing Technologies, Erice, Italy, July 1-13, 1991.
- 50. R. A. Batchelor and A. Hamnett, in Modern Aspects of Electrochemistry, J. O'M. Bockris et al., Eds., Plenum Press, New York, 1992, p. 265.
- 51. H. F. Okorn-Schmidt, I. Teerlinck, S. Biesemans, and M. M. Heyns, Proceedings of the Symposium on Environmental Aspects of Electrochemical Technology: Applications in Electronics, The Electrochemical Society, Pennington, NJ, 1997, p. 140.
- 52. E. P. Boonekamp, J. J. Kelly, J. van de Ven, and A. H. M. Sondag, J. Appl. Phys. 75, 8121 (1994).
- 53. D. Tonova, M. Depas, and J. Vanhellemont, Thin Solid Films 288, 64 (1996).
- 54. E. Kamieniecki and G. Foggiato, in Handbook of Semiconductor Wafer Cleaning Technology, W. Kern, Ed., Noves Publications, Park Ridge, NJ, 1993, p. 497.
- 55. N. F. Mott, Trans. Faraday Soc. 39, 472 (1940).
- 56. M. B. Brodsky and D. Cubicciotti, J. Amer. Chem. Soc. 73, 3497 (1951).
- 57. H. Gerischer and M. Lübke, Ber. Bunsenges. Phys. Chem. 92, 573 (1988).
- 58. L. Torcheux, A. Mayeux, and M. Chemla, J. Electrochem. Soc. 142, 2037 (1995).
- 59. V. Bertagna, C. Plougonven, F. Rouelle, and M. Chemla, J. Electrochem. Soc. 143, 3532 (1996).

- 60. V. Bertagna, C. Plougonven, F. Rouelle, and M. Chemla, J. Electroanal. Chem. 422, 115 (1997).
- 61. D. Gräf, M. Grundner, and R. Schulz, J. Vac. Sci. Technol. A 7, 808 (1989).
- V. Raghavan and M. Cohen, in Treatise on Solid State Chemistry, Vol. 5, N. B. Hannay, Ed., Plenum Press, New York, 1975, p. 67.
- 63. O. M. R. Chyan, J.-J. Chen, H.-Y. Chien, J. W. Wu, M. Liu, J. A. Sees, and L. H. Hall, J. Electrochem. Soc. 143, L235 (1996).
- 64. O. M. R. Chyan, J.-J. Chen, L. Chen, and F. Xu, J. Electrochem. Soc. 144, L17 (1997).
- 65. E. A. Kneer and S. Raghavan, Proceedings of the 5th International Symposium on Cleaning Technology in Semiconductor Device Manufacturing, 97-35, The Electrochemical Society, Pennington, NJ, 1998, p. 377.

Received November 2, 1998; accepted for publication February 22, 1999

Harald F. Okorn-Schmidt IBM Research Division, Thomas J. Watson Research Center, P.O. Box 218, Yorktown Heights, New York 10598 (hschmidt@us.ibm.com). Dr. Okorn-Schmidt joined IBM as a Research Staff Member at the Thomas J. Watson Research Center in 1996 after receiving a Ph.D. degree in chemical engineering from Graz University of Technology, Graz, Austria. From 1992 to 1996, while pursuing his Ph.D. degree, he was a Research Staff Member at IMEC, Leuven, Belgium, working in the Ultra Clean Processing Technology group of Dr. Marc Heyns. From 1987 through 1991 he was an associated student with the Siemens Research and Development facility in Munich, Germany, working in the Technology Characterization group of Dr. Bernd O. Kolbesen. Dr. Okorn-Schmidt's research interests include the impact of the surface chemistry, passivation, and photoelectrochemistry of silicon on advanced gate dieletrics, the electrochemical characterization of advanced gate dielectrics, and process integration.